10. Jäger, C. *et al.* Steps toward interstellar silicate mineralogy IV. The crystalline revolution. *Astron. Astrophys.* **339,** 904–916 (1998).
11. Molster, F. J. *et al.* Low-temperature crystallization of silicate dust in circumstellar disks. *Nature* **401,** 563–565 (1999).
12. Kessler, M. F. *et al.* The Infrared Space Observatory (ISO) mission. *Astron. Astrophys.* **315,** L27–L31 (1996).
13. Lester, D. F. & Dinerstein, H. L. An infrared disk at the center of the bipolar planetary nebula NGC 6302. *Astrophys. J.* **281,** L67–L69 (1984).
14. Corradi, R. L. M. & Schwarz, H. E. The kinematics of the high velocity bipolar nebulae NGC 6537 and HB 5. *Astron. Astrophys.* **269,** 462–468 (1993).
15. Gonzalez-Alfonso, E. & Cernicharo, J. The water vapor abundance in circumstellar envelopes. *Astrophys. J.* **525,** 845–862 (1999).
16. Payne, H. E., Philips, J. A. & Terzian, Y. A young planetary nebula with OH molecules—NGC 6302. *Astrophys. J.* **326,** 368–375 (1988).
17. Metzler, K., Bisschoff, A. & Stoeffler, D. Accretionary dust mantles in CM chondrites—Evidence for solar nebula processes. *Geochim. Cosmochim. Acta* **56,** 2873–2897 (1992).
18. Pottasch, S. R. & Beintema, D. A. The ISO spectrum of the planetary nebula NGC 6302. II. Nebular abundances. *Astron. Astrophys.* **347,** 975–982 (1999).
19. Rietmeijer, F. J. M. A model for diagenesis in proto-planetary bodies. *Nature* **313,** 293–294 (1985).
20. Lancet, M. S. & Anders, E. Carbon isotope fractionation in the Fischer-Tropsch synthesis and in meteorites. *Science* **170,** 980–982 (1970).
21. Pope, K. O., Ocampo, A. C., Fischer, A. G., Morrison, J. & Sharp, Z. Carbonate condensates in the Chicxulub ejecta deposits from Belize. *Lunar Planet. Sci.* **27,** 1045–1046 (1996).
22. Molster, F. J. *et al.* The complete ISO spectrum of NGC6302. *Astron. Astrophys.* **372,** 165–172 (2001).
23. Koike, C. *et al.* The spectra of crystalline silicates in infrared region. *Proc. 32nd ISAS Lunar Planet. Symp.* **32,** 175–178 (1999).
24. Koike, C. *et al.* Absorption spectra of Mg-rich Mg-Fe and Ca pyroxenes in the mid- and far-infrared regions. *Astron. Astrophys.* **363,** 1115–1122 (2000).
25. Bertie, J. E., Labbé, H. J. & Whalley, E. Absorptivity of Ice I in the range 4000-30 cm^{-1}. *J. Chem. Phys.* **50,** 4501–4520 (1969).
26. Warren, S. G. Optical constants of ice from the ultraviolet to the microwave. *Appl. Opt.* **23,** 1206–1225 (1984).
27. Jäger, C., Mutschke, H., Begemann, B., Dorschner, J. & Henning, Th. Steps toward interstellar silicate mineralogy I. Laboratory results of a silicate glass of mean cosmic composition. *Astron. Astrophys.* **292,** 641–655 (1994).
28. Henning, Th. & Stognienko, R. Dust opacities for protoplanetary accretion disks: influence of dust aggregates. *Astron. Astrophys.* **311,** 291–303 (1996).

Acknowledgements

This work is based on observations with ISO, an ESA project with instruments funded by ESA member states (especially the PI countries: France, Germany, the Netherlands and the UK) and with the participation of ISAS and NASA. We thank F. J. M. Rietmeijer, D. Fabian, J. Bouwman, C. Dominik, A. G. G. M. Tielens, J. Bradley, W. Schutte, J. Keane, P. Morris, L. P. Keller, H. Y. McSween Jr and R. N. Clayton for support and discussions. We acknowledge support from an NWO 'Pionier' grant.

Correspondence and requests for materials should be addressed to F.K. (e-mail: ciska@science.uva.nl).

Quantum states of neutrons in the Earth's gravitational field

Valery V. Nesvizhevsky*, Hans G. Börner*, Alexander K. Petukhov*, Hartmut Abele†, Stefan Baeßler†, Frank J. Rueß†, Thilo Stöferle†, Alexander Westphal†, Alexei M. Gagarski‡, Guennady A. Petrov‡ & Alexander V. Strelkov§

* *Institute Laue-Langevin, 6 rue Jules Horowitz, Grenoble F-38042, France*
† *University of Heidelberg, 12 Philosophenweg, Heidelberg D-69120, Germany*
‡ *Petersburg Nuclear Physics Institute, Orlova Roscha, Gatchina, Leningrad reg. R-188350, Russia*
§ *Joint Institute for Nuclear Research, Dubna, Moscow reg. R-141980, Russia*

The discrete quantum properties of matter are manifest in a variety of phenomena. Any particle that is trapped in a sufficiently deep and wide potential well is settled in quantum bound states. For example, the existence of quantum states of electrons in an electromagnetic field is responsible for the structure of atoms[16], and quantum states of nucleons in a strong nuclear field give rise to the structure of atomic nuclei[17]. In an analogous way, the gravitational field should lead to the formation of quantum states. But the gravitational force is extremely weak compared to the electromagnetic and nuclear force, so the observation of quantum states of matter in a gravitational field is extremely challenging. Because of their charge neutrality and long lifetime, neutrons are promising candidates with which to observe such an effect. Here we report experimental evidence for gravitational quantum bound states of neutrons. The particles are allowed to fall towards a horizontal mirror which, together with the Earth's gravitational field, provides the necessary confining potential well. Under such conditions, the falling neutrons do not move continuously along the vertical direction, but rather jump from one height to another, as predicted by quantum theory[1–3].

In order to allow for the experimental observation of gravitational bound states, all interactions of the matter particles with other fields must be so small that their interference with the gravitational quantum phenomena can be neglected. The choice of neutrons seemed to us most favourable because (1) they are neutral, (2) they have a long lifetime, and (3) they are elementary particles with low mass. The reasons why these properties are advantageous will become more evident from the following explanations.

We now consider how to demonstrate that bound states exist for neutrons trapped in the Earth's gravitational field. The gravitational field alone does not create a potential well, as it can only confine particles by forcing them to fall along gravity field lines. We need a second 'wall' to create the well. This can be obtained by introducing a reflecting mirror. Let us consider a neutron, which is lifted up by a few millimetres and is then dropped vertically onto the mirror. The neutron wave is reflected by the mirror and interferes with itself, as illustrated in Fig. 1. This self-interference creates a standing wave in the neutron density: the probability of finding a neutron at a given height exhibits maxima and minima along the vertical direction, the position of which depends on the quantum number of the bound states. The neutron that was dropped has gone through quantum 'steps'.

The classical analogue, the vibrating musical string, gives a visualization of a particle in a rectangular potential well. In this case, strict boundary conditions must be met: both the wavefunction amplitudes of the particles and the displacement amplitudes of the string vanish at the boundaries. In contrast, the gravitational well described above is asymmetric: whereas the reflecting mirror (under total reflection condition) corresponds to an infinite sharp

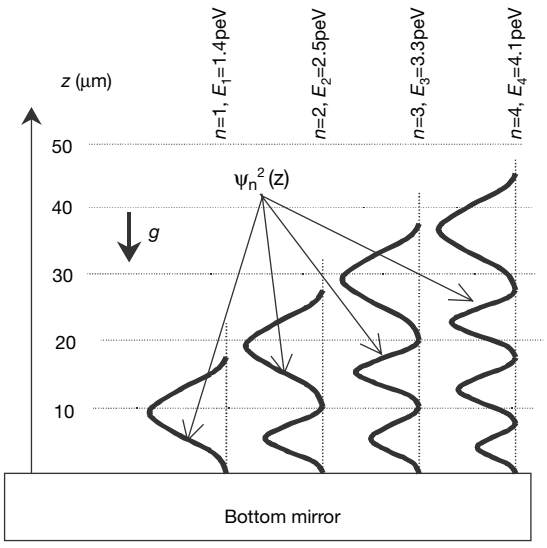

Figure 1 Wavefunctions of the quantum states of neutrons in the potential well formed by the Earth's gravitational field and the horizontal mirror. The probability of finding neutrons at height z, corresponding to the nth quantum state, is proportional to the square of the neutron wavefunction $\psi_n^2(z)$. The vertical axis z provides the length scale for this phenomenon. E_n is the energy of the nth quantum state.

wall, the gravitational field is much softer; as a result, the gravitational well extends in the opposite direction to the gravity field with increasing quantum number. Consequently, as can be seen in Fig. 1, the neutron wavefunctions are deformed upwards, and the energy differences between states with neighbouring quantum numbers become smaller with increasing level number. More detailed discussions, precise analytical solutions and related publications can be found elsewhere[1–10]. We will here simply summarize the results of these analyses: the energies of the four lowest quantum states of a neutron in the Earth's gravitational field are $E_1 \approx 1.41$ peV, $E_2 \approx 2.46$ peV, $E_3 \approx 3.32$ peV and $E_4 \approx 4.08$ peV, respectively (1 peV $= 10^{-12}$ eV). It is worth keeping in mind that the classical energy that is needed to lift a neutron by 10 μm against gravitation on Earth (given by mgz) is almost exactly 1 peV. (Here m is the neutron mass, g is the acceleration due to gravity, and z is the height.) Thus the energy E_1 corresponds in the classical approximation to the height $z_1 \approx 15$ μm, at which the first level of the quantum phenomenon for neutrons should be observed. This 'macroscopic' height is very advantageous, and helps us to design experiments to demonstrate the existence of gravitational levels for neutrons.

In a realistic experiment it is not possible to just lift a neutron, let it drop, and then measure its density distribution as a function of height. But we can take a beam of neutrons and let them fly horizontally above a reflecting mirror. If all forces can be eliminated except for gravitation and repulsion by the mirror (such as that due to magnetic field gradients, mechanical vibrations and so on), then the motion of the neutrons can be decoupled into independent vertical and horizontal components. The gravitational force acts on the vertical component only, and in this direction we then obtain the potential well that leads to the consequences described above. No forces act on the horizontal velocity component.

In order to further characterize our experiment, we have to make use of the uncertainty principle, which relates the Plank constant ($\hbar = 6.6 \times 10^{-16}$ eV s) to the minimal time period $\Delta\tau$, during which quantum states can be resolved with an energy difference $\Delta E : \Delta\tau \approx \hbar/\Delta E$. Therefore, the vertical energy scale of the quantum levels $E_1 \approx 1.41$ peV requires that $\Delta\tau \gg 0.5$ ms. A compromise has to be found between the length of the reflecting mirror and the horizontal velocity of neutrons. We have used mirrors with a length of 10 cm, and neutrons with a velocity of ~ 10 m s^{-1}. A powerful source of ultracold neutrons (UCN)[11–14], which operates at the Institute Laue-Langevin, Grenoble[15], provides the neutrons with such velocity. The energy E_1 corresponds in the classical approximation to the vertical velocity component $v \approx 1.7$ cm s^{-1}, which is significantly smaller than the horizontal velocity component. If we let the neutrons fly 'slightly upwards' (see Fig. 2), they will follow a parabolic trajectory due to gravity. At the maximum of the parabola their vertical velocity component will be zero in the classical approximation, and will then increase again. To limit the vertical velocity component, we use an absorber parallel to the bottom mirror and placed above it (see Fig. 2). The distance between absorber and mirror can be adjusted.

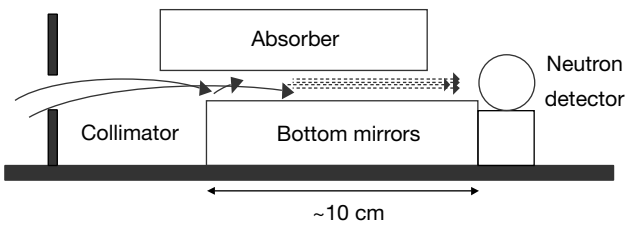

Figure 2 Layout of the experiment. The limitation of the vertical velocity component depends on the relative position of the absorber and mirror. To limit the horizontal velocity component we use an additional entry collimator. The relative height and size of the entry collimator can be adjusted.

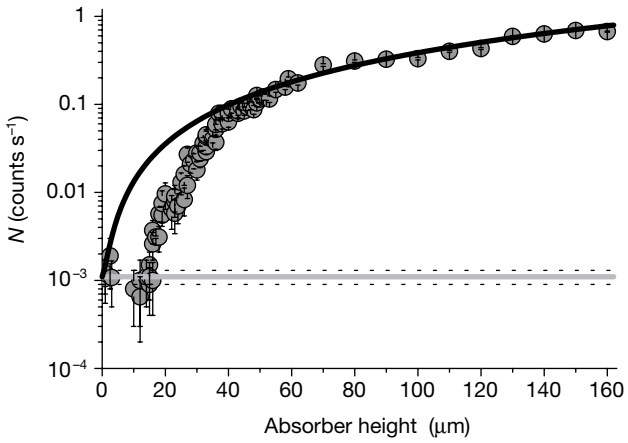

Figure 3 The neutron throughput N versus the absorber height. The circles represent the data points. The solid curve is the classical fit to these data. The slit becomes transparent to neutrons at a finite slit opening. The horizontal straight lines indicate the detector background values and uncertainties measured while the neutron source was 'off'.

In our experiments, neutrons flow between the mirror below and absorber above, and the neutron transmission N is measured as a function of the width Δz of the slit defined by the mirror and the absorber. This width Δz acts as a selector for the vertical velocity component. In order to keep the vertical and horizontal velocity components decoupled, severe restrictions concerning quality and adjustment of the different parts used in the set-up must be met[2,3]. Ideally, from Fig. 1, we expect a stepwise dependence of N as a function of Δz. If Δz is smaller than the spatial width of the lowest quantum state, then N should be zero. When Δz is equal to the spatial width of the lowest quantum state, then N should increase sharply. Further increase in Δz should not increase N as long as Δz is smaller than the spatial width of the second quantum state. Then, N should again increase stepwise. At sufficiently large slit width Δz, the classical dependence $N \sim \Delta z^{1.5}$ should be approached, and the stepwise increase should be washed out. (Naively we might expect that classically $N \sim \Delta z$; this is not the case because we obtain an additional $z^{0.5}$ due to the fact that an increase in Δz also allows for an increase in the accepted spread of velocities.) The identification of the lowest quantum state is easier than that of the higher states because in this case the relative change in the count rate N is maximal.

The effects that we observe, shown in Fig. 3, are consistent with the expectations described above. In particular, the non-transparency of the slit (formed by the bottom mirror and the absorber) is clearly observed for the neutrons when the slit width is smaller than the spatial width of the lowest quantum state. We note that the 'diameter' of a neutron is $\sim 10^{-13}$ cm, which is much smaller than the width of ≥ 15 μm at which the slit starts to become transparent for neutrons. Careful analysis of the experiment has allowed us to rule out any systematic errors. In particular, tests have shown that the shape of the transmission curve (Fig. 3) does not depend on the value of the horizontal velocity component, but that it depends only on the vertical velocity component, as expected. If the slit is opened up to 15 μm, it is just not transparent for neutrons. But it is sufficiently large that we can observe transmission of visible light, although the wavelength of light (~ 0.6 μm) is much larger than the neutron wavelength of ~ 0.01 μm; this observation tells us that the slit is really open and well adjusted. Evidently, the difference in transmission results from the fact that the Earth's gravitational field does not act noticeably on photons within the frame of our experimental set-up.

Figure 4 shows on an extended scale the initial part of the transmission curve N as a function of slit width Δz. The dashed

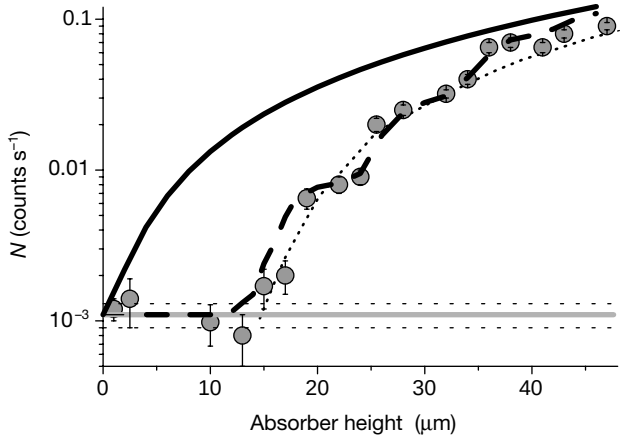

Figure 4 The neutron throughput versus the absorber height at low height values. The data points are summed up in intervals of 2 μm. The dashed curve corresponds to a fit using the quantum-mechanical calculation, in which all level populations and the height resolution are fitted from the experimental data. The solid curve is again the full classical treatment. The dotted line is a truncated fit in which it is assumed that only the lowest quantum state—which leads to the first step—exists.

curve shows the results of a quantum fit, in which the level populations and the height resolution are free parameters. The solid line is again the full classical treatment ($N \sim z^{1.5}$). The dotted line is a truncated fit to the assumption that only the lowest quantum level—which leads to the first step—exists. Then it continues at the absorber height of $z_1 \approx 15\,\mu m$ with a shifted classical treatment ($N \sim (z - z_1)^{1.5}$) that is more like a 'guide to the eye' curve. Our statistics for large slit width are still not sufficient, but the existence of the first step due to the lowest quantum level is clearly reproduced.

Our experimental observations of the neutron quantum states in the Earth's gravitational field provide another demonstration of the universality of the quantum properties of matter, but at this stage we have only shown a phenomenon that was expected—although not easy to prove. As the parameters of quantum states are defined in such a system mainly by the interaction of the neutron with the gravitational field, the phenomenon we report can now be considered for further investigations of fundamental properties of matter. Thus, as it is evident from the uncertainty principle, the energy resolution ΔE could be improved significantly by increasing $\Delta\tau$ (in principle, ΔE could be as low as $\sim 10^{-18}$ eV if $\Delta\tau$ approaches the lifetime of the neutron, so that the level width becomes a million times smaller than the energy difference between levels). The use of resonance transitions between such narrow levels could find applications in physics, such as the precise verification of the proportionality of inertial and gravitational masses of elementary particles (neutrons), and a check of the electrical neutrality of neutrons—which is not a trivial fact. Increasing the time that neutrons spend in the gravitational bound states will become one of the main challenges in extending this experiment. When trying to achieve this, it will be necessary to demonstrate that the neutrons are spending a much longer time in the potential well, and a significant increase in the available density of ultracold neutrons will be necessary. □

Received 10 October; accepted 22 November 2001.

1. Luschikov, V. I. & Frank, A. I. Quantum effects occurring when ultracold neutrons are stored on a plane. *JETP Lett.* **28,** 559–561 (1978).
2. Nesvizhevsky, V. V. *et al.* Search for quantum states of the neutron in a gravitational field: gravitational levels. *Nucl. Instrum. Methods Phys. Res.* **440,** 754–759 (2000).
3. Nesvizhevsky, V. V. *et al.* in *ILL Annual Report* (eds Cicognani, G. & Vettier, Ch.) 64–65 (Institute Laue-Langevin, Grenoble, 2000).
4. Landau, L. D. & Lifshitz, E. M. *Quantum Mechanics* 164–196 (Pergamon, Oxford, 1976).
5. Flügge, S. *Practical Quantum Mechanics* (Mir, Moscow, 1974).
6. Colella, R. A., Overhauser, W. & Werner, W. A. Observation of gravitationally induced quantum interference. *Phys. Rev. Lett.* **34,** 1472–1474 (1975).
7. Baryshevskii, V. G., Chrerepitza, S. V. & Frank, A. I. Neutron spin interferometry. *Phys. Lett. A* **153,** 299–302 (1991).
8. Frank, A. I. Modern optics of long-wavelength neutrons. *Sov. Phys. Usp.* **34,** 980–987 (1991).
9. Felber, J., Gähler, R., Rauch, C. & Golub, R. Matter waves at a vibrating surface: Transition from quantum-mechanical to classical behavior. *Phys. Rev. A* **53,** 319–328 (1996).
10. Peters, A., Chung, K. Y. & Chu, S. Measurement of gravitational acceleration by dropping atoms. *Nature* **400,** 849–852 (1999).
11. Luschikov, V. I., Pokotilovsky, Yu. N., Strelkov, A. V. & Shapiro, F. L. Observation of ultracold neutrons. *JETP Lett.* **9,** 23–26 (1969).
12. Steyerl, A. Measurement of total cross sections for very slow neutrons with velocities from 100m/s to 5m/s. *Phys. Lett. B* **29,** 33–35 (1969).
13. Ignatovich, V. K. *The Physics of Ultracold Neutrons* (Clarendon, Oxford, 1990).
14. Golub, R., Richardson, D. J. & Lamoreux, S. K. *Ultracold Neutrons* (Higler, Bristol, 1991).
15. Steyerl, A. & Malik, S. S. Sources of ultracold neutrons. *Nucl. Instrum. Methods Phys. Res. A* **284,** 200–207 (1989).
16. Born, M. *Atomic Physics* (Blackie & Son, London, 1969).
17. Bohr, A. & Mottelson, B. R. *Nuclear Structure* (Benjamin, New York, 1969).

Acknowledgements

We are grateful to our colleagues who were interested in this research and contributed to its development, in particular K. Ben-Saidane, D. Berruyer, Th. Brenner, J. Butterworth, D. Dubbers, P. Geltenbort, T. M. Kuzmina, A. J. Leadbetter, B. G. Peskov, S. V. Pinaev, K. Protasov, I. A. Snigireva, S. M. Soloviev and A. Voronin. The work was supported by INTAS.

Competing interests statement

The authors declare that they have no competing financial interests.

Correspondence and requests for materials should be addressed to V.V.N. (e-mail: nesvizhevsky@ill.fr).

Antiferromagnetic order induced by an applied magnetic field in a high-temperature superconductor

B. Lake*†, H. M. Rønnow‡, N. B. Christensen§‖, G. Aeppli§¶, K. Lefmann§, D. F. McMorrow§, P. Vorderwisch#, P. Smeibidl#, N. Mangkorntong☆, T. Sasagawa☆, M. Nohara☆, H. Takagi☆ & T. E. Mason**

** Oak Ridge National Laboratory, PO Box 2008 MS 6430, Oak Ridge, Tennessee 37831-6430, USA*
† Department of Condensed Matter Physics, University of Oxford, Clarendon Laboratory Parks Road, Oxford OX1 3PU, UK
‡ CEA (MDN/SPSMS/DRFMC), 17 Ave. des Martyrs, 38054 Grenoble cedex 9, France
§ Materials Research Department, Risø National Laboratory, 4000 Roskilde, Denmark
‖ Ørsted Laboratory, Niels Bohr Institute for APG, Universitetsparken 5, DK 2100, Copenhagen, Denmark
¶ NEC Research Institute, 4 Independence Way, Princeton, New Jersey 08540-6634, USA
 # BENSC, Hahn-Meitner Institut, Glienicker Strasse 100, 14109 Berlin, Germany
☆ Department of Advanced Materials Science, Graduate School of Frontier Sciences, University of Tokyo, Hongo 7-3-1, Bunkyo-ku, Tokyo 113-8656, Japan
*** Experimental Facilities Division, Spallation Neutron Source, 701 Scarboro Road, Oak Ridge, Tennessee 37830, USA*

One view of the high-transition-temperature (high-T_c) copper oxide superconductors is that they are conventional superconductors where the pairing occurs between weakly interacting quasiparticles (corresponding to the electrons in ordinary metals), although the theory has to be pushed to its limit[1]. An alternative view is that the electrons organize into collective textures (for example, charge and spin stripes) which cannot be 'mapped' onto the electrons in ordinary metals. Understanding the properties of the material would then need quantum field theories of objects